



OPEN

Biodegradability and biocompatibility test of Magnesium Carbonate apatite composite implants fabricated by extrusion technique on Sprague Dawley Rats

Achmad Fauzi Kamal¹, Eugene Dionysios¹✉, Sugeng Supriadi², Iwan Setyadi³, Vtnizah Juniantito⁴ & Ahmad Jabir Rahyussalim¹

Background and purpose Magnesium (Mg) has a biomechanical character resembling bone, with mechanical strength exceeding that of ceramics, but has a high corrosion rate. One method to reduce the corrosion level of Mg is to mix it with other materials or coatings. Carbonate apatite (CA) was chosen as a Mg composite mixture because of its good osteoconductivity, and this study aimed to evaluate the biodegradability of MgxCa composite implants made by the extrusion technique in Sprague Dawley (SD) rats. **Methods** This study was a post-test only *in vivo* experiment in SD rats from July to December 2021. Thirty SD rats were divided into five treatment groups: Mg0CA, Mg5CA, Mg10CA, Mg15CA, and titanium plates. The examination included implant weight changes, postoperative gas formation, and local and systemic histopathological analyses on days 15 and 30. **Results** There was a significant difference in gas formation on day 15 and implant degeneration between groups ($p < 0.05$). However, in post-hoc analysis, we found no significant differences in implant weight difference or implant gas production between pre- and post-sacrifice in the MgxCa composites ($p > 0.05$). **Histopathological examination** revealed no significant local or systemic inflammatory response differences between groups ($P > 0.05$). **Conclusion** The combination of magnesium with apatite carbonate from extruded fabrication techniques is a biodegradable implant with biocompatibility and nontoxic properties, either locally or systemically.

Keywords Biodegradable, Magnesium Carbonate, Carbonate apatite, Extrusion techniques

Biodegradable orthopaedic implants have rapidly developed, reducing removal morbidity. Magnesium, a biomechanical material with human bone properties, is a viable option but is highly corrosive. (1) Mixing magnesium alloy with other materials reduces the corrosion rate. (2) Carbonate apatite is commonly used in orthopaedic implants because of its non-organic, osteoconductive nature. (3) Despite the advantages of the magnesium carbonate apatite (MgCA) alloy, the alloy is degraded rapidly, thus leading to the weakening of the implant. (3) The corrosion process of MgCA alloy is related to the low density of MgCA alloy. (4) Modification in fabrication techniques through milling, sintering, and extrusion can improve MgCA alloy density. Extrusion offers dense compaction and a lower corrosion rate, while milling technique shows good biocompatibility. (5).

Results from an *in vitro* study of MgCA alloy wire produced using the extrusion technique have low toxicity to normal human cells. (6) However, results regarding biodegradation from *in vitro* and *in vivo* studies may differ. A study by Antoniac et al. comparing the biodegradability of Mg-1Ca magnesium alloys *in vitro* and *in vivo* found contradicting finding regarding the corrosion and cytotoxicity results. (7) There has been no prior *in vivo* biodegradability study of MgCA. This study aimed to evaluate the biodegradability and bioavailability of MgCA alloy fabricated using the extrusion technique as an implant in SD rats.

¹Department Orthopedic and Traumatology, Faculty of Medicine, Universitas Indonesia, Cipto Mangunkusumo General Hospital, Jakarta 10430, Indonesia. ²Department of Mechanical Engineering, Faculty of Engineering, Universitas Indonesia, Depok 16424, Indonesia. ³Department of Metallurgical and Materials Engineering, Faculty of Engineering, Universitas Indonesia, Depok 16424, Indonesia. ⁴Department of Veterinary Pathology, Bogor Agricultural University, Bogor, Indonesia. ✉email: eugene.dionysios@gmail.com

Results

In this study, we conducted an experimental test in 30 SD rats divided into five research groups. The sacrifice period for histopathological examination was conducted in two stages, namely at 15 days post-operation and 30 days post-operation. Characteristics of the samples included a median body weight of 295.5 g (lowest weight of 228 g and highest weight of 360 g). The average implant weight was 30 mg, with a minimum weight of 20 mg and a maximum weight of 125 mg. Complications were observed in 17 (56.6%) research samples, with the majority experiencing mild non-suppurative nephritis (60%), followed by mild focal portal hepatitis (6.7%), and mild white pulp hyperplasia (3.3%) on histopathological examination. (Table 1).

Post-operative hematological tests for systemic inflammation results showed no significant difference between groups. (Table 2) The local histopathological examination of inflammatory cell infiltration, connective tissue scoring, neovascularization scoring, number of osteoclast cells, and osteoblast activity showed no significant differences between the groups (Table 3).

In this study, the difference in implant weight before and after sacrifice was evaluated. The comparative analysis results showed significant differences in implant weight between the groups (Table 4; Fig. 1). Post-hoc analysis showed a significant difference between MgCA implants and titanium but no significant differences between MgCA compositions. (Table 5). The degradation rate described in this study is as follows: On the 15 days observation, the Mg0CA rate was 5.48 mg/day, Mg5CA was 5.68 mg/day, Mg10CA was 4.55 mg/day, Mg15CA was 3.46 mg/day. While on the 30 days observation, the rate of degradation were slower with Mg0CA of 2.68 mg/day, Mg5CA of 3.01 mg/day, Mg10CA of 2.42 mg/day, and Mg15CA of 1.82 mg/day. From the results, we can see that the higher the CA content, the slower the rate of implant degradation.

Implant gas production was also measured by obtaining the volume of peri-implant gas using radiography (Table 6; Fig. 2). The results showed a significant difference in gas production between groups on day 15. However, post-hoc analysis showed significant differences between MgCA implants and titanium implants, but no significant differences were observed between MgCA compositions.

Discussion

Progress in the development of implants and orthopaedic devices has led to the need for biodegradable implants with less implant removal morbidity and comfort for patients. Magnesium implants have been recognized as a potential material for biodegradable implants. However, the rapid degradation rate of the material in physiological fluid leads to the weakening of the implant. MgCA is a magnesium alloy that can decrease the degradation rate of magnesium implants. In this study, we aimed to demonstrate the biocompatibility and biodegradability of MgCA implants *in vivo* using an animal model.

Magnesium is an important chemical macronutrient (comprising 0.2% of the human body weight), which has good biocompatibility and biodegradability, as well as high tensile strength compared to polymers and is less brittle than ceramics. The elastic modulus of magnesium (45 GPa) is closer to the elastic modulus of cortical bone (15–25 GPa) than the elastic moduli of titanium alloys and stainless steel (115–200 GPa). (8) Due to high degenerative rate inside the body, magnesium is combined with carbonate apatite to enhance its strength and decrease its degeneration rate. (2), (9), (10) Magnesium carbonate apatite (MgCA) is chemically related to hydroxyapatite, the major mineral component of bone. (11) Thus, orthopaedic implants composed of materials such as MgCA can aid in bone repair. These compounds have been shown to encourage the development of new bone tissues, implying that they can aid in bone repair and regeneration. Due to its unique characteristics such as biocompatibility, osteoconductivity, and biodegradability, this MgCA is an attractive material to be used in orthopaedic implant. (12) In this study, we conducted an extrusion method of mixing magnesium with carbonate apatite, which has several advantages, including higher implant density, enhanced biocompatibility, and increased resistance to wear and tear.

Group	n(%) / Median (min-max)
Titanium	6 (20)
Mg0%CA	6 (20)
Mg5%CA	6 (20)
Mg10%CA	6 (20)
Mg15%CA	6 (20)
Body weight (gram)	295.5 (228–360)
Implant weight (mg)	30 (20–125)
Sacrifice Time	
Day 15	15 (50)
Day 30	15 (50)
Complication	17 (56.6)
Mild non-suppurative interstitial nephritis	18 (60)
Mild focal portal hepatitis	2 (6.7)
Mild white pulp hyperplasia	1 (3.3)

Table 1. Sample characteristics.

	Implant										
		Titanium	p	Mg0CA	Nilai p	Mg5CA	Nilai p	Mg10CA	Nilai p	Mg15CA	Nilai p
Hb	Pre	14.9 (\pm 1.82)	0,898	14.9 (\pm 0.99)	0,033	14.5 (\pm 0.25)	0,466	15.1 (\pm 0.65)	0,295	14.6 (\pm 1.36)	0,981
	Post	13.8 (\pm 1.51)		14.6 (\pm 0.83)		14.1 (\pm 0.56)		13.4 (\pm 1.52)		14.5 (\pm 0.99)	
RBC	Pre	8.42 (\pm 1.22)	0,797	8.28 (\pm 0.62)	0,292	8.56 (\pm 0.52)	0,639	8.67 (\pm 0.28)	0,963	8.09 (\pm 0.60)	0,637
	Post	7.53 (\pm 0.69)		8.00 (\pm 0.30)		8.04 (\pm 0.68)		7.52 (\pm 0.71)		7.95 (\pm 0.54)	
Ht	Pre	46.7 (\pm 7.51)	0,735	46.4 (\pm 2.36)	0,979	47.1 (\pm 3.14)	0,081	47.5 (\pm 2.14)	0,247	45.5 (\pm 3.49)	0,763
	Post	40.8 (\pm 3.65)		45.1 (\pm 2.02)		43.6 (\pm 1.74)		40.5 (\pm 4.41)		44.5 (\pm 2.92)	
MCV	Pre	55.3 (\pm 1.27)	0,373	57.3 (\pm 1.81)	0,275	55.1 (\pm 2.61)	0,415	54.8 (\pm 2.07)	0,371	56.3 (\pm 1.88)	0,597
	Post	54.3 (\pm 0.45)		56.5 (\pm 1.49)		54.5 (\pm 2.93)		53.9 (\pm 1.04)		56.1 (\pm 0.87)	
MCH	Pre	17.7 (\pm 0.75)	0,308	18.0 (\pm 0.98)	0,457	16.9 (\pm 1.07)	0,156	17.3 (\pm 0.97)	0,310	18.1 (\pm 1.37)	0,931
	Post	18.2 (\pm 0.86)		18.3 (\pm 0.88)		17.5 (\pm 1.30)		17.4 (\pm 0.58)		16.6 (\pm 4.48)	
MCHC	Pre	32.1 (\pm 1.43)	0,081	31.6 (\pm 1.56)	1,000	30.9 (\pm 1.93)	0,049	31.8 (\pm 2.25)	0,114	32.2 (\pm 2.91)	0,939
	Post	33.7 (\pm 1.39)		32.5 (\pm 1.00)		32.3 (\pm 0.94)		32.9 (\pm 0.95)		32.6 (\pm 1.18)	
RDW	Pre	13.2 (\pm 1.29)	0,182	13.3 (\pm 2.99)	0,364	12.6 (\pm 1.09)	0,006	12.9 (\pm 1.02)	0,300	13.1 (\pm 1.42)	0,284
	Post	12.8 (\pm 1.09)		13.5 (\pm 2.01)		13.1 (\pm 0.59)		14.0 (\pm 0.92)		13.1 (\pm 0.97)	
Thrombocyte	Pre	898.33 (\pm 585.64)	0,053	1129.5 (\pm 510.82)	0,327	1316.6 (\pm 316.23)	0,131	1244.6 (\pm 206.14)	0,127	1116 (\pm 200.51)	0,527
	Post	668.83 (\pm 351.89)		974.8 (\pm 184.29)		1019.3 (\pm 348.47)		567.16 (\pm 446.56)		981 (\pm 238.84)	
PCT	Pre	0.36 (\pm 0.16)	0,915	0.53 (\pm 0.21)	0,659	0.60 (\pm 0.06)	0,154	0.56 (\pm 0.08)	0,947	0.59 (\pm 0.07)	0,639
	Post	0.34 (\pm 0.18)		0.50 (\pm 0.11)		0.52 (\pm 0.16)		0.55 (\pm 0.59)		1.31 (\pm 2.09)	
MPV	Pre	5.38 (\pm 0.21)	0,183	5.38 (\pm 0.25)	0,118	5.36 (\pm 0.58)	0,096	5.15 (\pm 0.33)	0,096	5.6 (\pm 0.57)	0,278
	Post	5.35 (\pm 0.64)		5.12 (\pm 0.42)		5.23 (\pm 0.47)		5.13 (\pm 0.40)		6.88 (\pm 4.48)	
PDW	Pre	16.2 (\pm 0.20)	0,938	16.1 (\pm 0.25)	0,903	16.1 (\pm 0.24)	0,916	15.9 (\pm 0.19)	0,825	15.5 (\pm 1.75)	0,876
	Post	16.4 (\pm 1.15)		15.9 (\pm 0.21)		16.0 (\pm 0.27)		16.3 (\pm 0.64)		15.6 (\pm 1.28)	
WBC	Pre	12.0 (\pm 4.40)	0,603	13.1 (\pm 6.20)	0,691	15.9 (\pm 5.72)	0,243	13.4 (\pm 5.15)	0,092	14.1 (\pm 6.59)	0,744
	Post	11 (\pm 3.36)		12.3 (\pm 3.61)		13.2 (\pm 3.34)		9.61 (\pm 3.47)		11.3 (\pm 3.24)	
Lymphocyte	Pre	7.63 (\pm 3.42)	0,350	8.38 (\pm 4.72)	0,225	8.68 (\pm 3.10)	0,036	6.95 (\pm 2.72)	0,520	8.7 (\pm 5.17)	0,322
	Post	6.58 (\pm 1.69)		7.24 (\pm 3.00)		7.33 (\pm 2.15)		5.16 (\pm 0.94)		5.96 (\pm 3.42)	
Monocyte	Pre	0.38 (\pm 0.13)	0,589	0.43 (\pm 0.22)	0,870	0.46 (\pm 0.23)	0,923	0.41 (\pm 0.21)	0,034	0.46 (\pm 0.22)	0,153
	Post	0.36 (\pm 0.15)		0.4 (\pm 0.14)		1.36 (\pm 2.37)		0.31 (\pm 0.13)		1.13 (\pm 1.75)	
Granulocyte	Pre	4.06 (\pm 1.20)	0,507	4.36 (\pm 2.18)	0,367	6.76 (\pm 3.54)	0,172	6.03 (\pm 2.68)	0,969	4.95 (\pm 2.40)	0,448
	Post	4.05 (\pm 1.94)		4.66 (\pm 1.29)		4.55 (\pm 2.94)		4.13 (\pm 2.55)		6.56 (\pm 5.25)	
ALP	Pre	29.6 (\pm 16.1)	0,314	26.6 (\pm 9.15)	0,075	26.5 (\pm 10.0)	0,002	37.5 (\pm 18.9)	0,781	27.5 (\pm 8.61)	0,986
	Post	38 (\pm 4.47)		36.5 (\pm 12.1)		37.2 (\pm 5.03)		38.1 (\pm 3.54)		35.5 (\pm 2.73)	
SGPT	Pre	23.6 (\pm 5.64)	0,033	32.8 (\pm 10.4)	0,868	39.6 (\pm 14.7)	0,024	37.1 (\pm 16.6)	0,185	40.8 (\pm 14.5)	0,048
	Post	26.5 (\pm 5.64)		37.8 (\pm 15.5)		41.8 (\pm 9.88)		34.1 (\pm 14.4)		38.1 (\pm 12.9)	
SGOT	Pre	55.1 (\pm 23.5)	0,026	69.6 (\pm 30.9)	0,692	78.1 (\pm 28.8)	0,829	79.3 (\pm 38.9)	0,390	61.8 (\pm 11.5)	0,868
	Post	40.8 (\pm 17.2)		63.8 (\pm 14.0)		59 (\pm 7.94)		50.3 (\pm 30.6)		45.5 (\pm 8.24)	
Total Protein	Pre	5.88 (\pm 0.33)	0,375	6.36 (\pm 0.73)	0,709	6.26 (\pm 0.67)	0,312	6.45 (\pm 0.71)	0,233	6.18 (\pm 0.54)	0,539
	Post	5.71 (\pm 0.80)		6.23 (\pm 0.45)		6.2 (\pm 0.50)		6.36 (\pm 0.58)		6.38 (\pm 0.51)	
Glucose	Pre	94.1 (\pm 35.5)	0,581	83.1 (\pm 30.2)	0,919	71.8 (\pm 21.2)	0,179	141. (\pm 128.)	0,586	84.3 (\pm 8.80)	0,605
	Post	90.3 (\pm 29.6)		95.1 (\pm 31.5)		87 (\pm 31.0)		90.6 (\pm 26.9)		97.5 (\pm 33.8)	
Ureum	Pre	18.5 (\pm 3.83)	0,684	20.1 (\pm 4.99)	0,085	19.1 (\pm 4.62)	0,766	18 (\pm 6.03)	0,815	18.3 (\pm 3.44)	0,384
	Post	19 (\pm 2.52)		21.8 (\pm 4.44)		19.8 (\pm 3.97)		18 (\pm 5.36)		20 (\pm 4.19)	
Creatinine	Pre	0.15 (0.1–0.2)	0,083	0.15 (0.1–0.3)	0,317	0.2 (0.1–0.3)	1,000	0.2 (0.1–0.4)	0,564	0.2 (0.1–0.3)	0,317
	Post	0.2 (0.1–0.3)		0.2		0.2 (0.1–0.2)		0.2 (0.2–0.3)		0.2 (0.2–0.3)	

Table 2. Comparison of hematological results of Mg0CA, Mg5CA, Mg10CA, Mg15CA, and titanium groups. Mean \pm SD; Median (Min-Max).

Biocompatibility profile of MgCA has been described in previous studies which reported high biocompatibility in living tissue.(5) In this study, we observed the local reaction of MgCA with various proportions of carbonate apatite compared to a titanium implant, with no significant difference. Local inflammation is a normal reaction to foreign objects owing to the innate immune response of the body. However, a biocompatible implant should not elicit severe inflammation, which can lead to alterations in bone healing. A previous study by Rahyussalim et al. has reported that the powder form of carbonate apatite cannot be used directly as a bone substitute because it triggers the formation of crystals from the inflammatory response.(5) However, fabrication into a plate using sintering or extrusion method could increase the density of the implant, thus reducing the risks

Parameters	None or minimal; <i>n</i> (%)	Mild; <i>n</i> (%)	Moderate; <i>n</i> (%)	Severe; <i>n</i> (%)	Very severe; <i>n</i> (%)	<i>P</i> value
Inflammatory cell infiltration						
Titanium	1 (16.7)	3 (50.0)	1 (16.7)	0 (0)	1 (16.7)	0.715
Mg0CA	0 (0)	2 (33.3)	1 (16.7)	1 (16.7)	2 (33.3)	
Mg5CA	1 (16.7)	2 (33.3)	0 (0)	0 (0)	3 (50.0)	
Mg10CA	0 (0)	2 (33.3)	1 (16.7)	2 (33.3)	1 (16.7)	
Mg15CA	0 (0)	3 (50.0)	2 (33.3)	0 (0)	1 (16.7)	
Soft tissue scoring						
Titanium	1 (16.7)	3 (50.0)	1 (16.7)	0 (0)	1 (16.7)	0.373
Mg0CA	0 (0)	0 (0)	3 (50.0)	2 (33.3)	1 (16.7)	
Mg5CA	0 (0)	3 (50.0)	0 (0)	0 (0)	3 (50.0)	
Mg10CA	0 (0)	2 (33.3)	1 (16.7)	2 (33.3)	1 (16.7)	
Mg15CA	0 (0)	1 (16.7)	5 (83.3)	0 (0)	0 (0)	
Neovascularization						
Titanium	1 (16.7)	3 (50.0)	1 (16.7)	0 (0)	1 (16.7)	0.505
Mg0CA	0 (0)	1 (16.7)	3 (50.0)	1 (16.7)	1 (16.7)	
Mg5CA	0 (0)	3 (50.0)	0 (0)	0 (0)	3 (50.0)	
Mg10CA	0 (0)	2 (33.3)	1 (16.7)	2 (33.3)	1 (16.7)	
Mg15CA	0 (0)	3 (50.0)	2 (33.3)	0 (0)	1 (16.7)	
Local osteoclast count						
Titanium	5 (83.3)	1 (16.7)	0 (0)	0 (0)	0 (0)	0.220
Mg0CA	2 (33.3)	2 (33.3)	1 (16.7)	1 (16.7)	0 (0)	
Mg5CA	0 (0)	3 (50.0)	1 (16.7)	2 (33.3)	0 (0)	
Mg10CA	3 (50.0)	1 (16.7)	1 (16.7)	1 (16.7)	0 (0)	
Mg15CA	5 (83.3)	0 (0)	0 (0)	0 (0)	0 (0)	
Osteoblast activity						
Titanium	1 (16.7)	3 (50.0)	1 (16.7)	1 (16.7)	0 (0)	0.468
Mg0CA	0 (0)	2 (33.3)	2 (33.3)	2 (33.3)	0 (0)	
Mg5CA	0 (0)	2 (33.3)	1 (16.7)	1 (16.7)	2 (33.3)	
Mg10CA	0 (0)	2 (33.3)	2 (33.3)	1 (16.7)	1 (16.7)	
Mg15CA	0 (0)	3 (50.0)	2 (33.3)	1 (16.7)	0 (0)	

Table 3. Local histopathological examination.

Group	15 days		30 days	
	Weight difference (gram)	<i>P</i> value	Weight difference (gram)	<i>P</i> value
Titanium	0	0.000	0	0.000
Mg0CA	82.3 ± 12.5		86 ± 13.1	
Mg5CA	85.3 ± 10.0		90.3 ± 11.0	
Mg10CA	68.3 ± 12.0		72.6 ± 10.6	
Mg15CA	52 ± 26.4		54.6 ± 19.1	

Table 4. Comparison analysis of the weight difference of implants in the Mg0CA, Mg5CA, Mg10CA, Mg15CA, and titanium groups. Mean ± SD.

of local inflammation.(11) Unfortunately, the sintering process requires high temperatures, which induce the decomposition of carbonate apatite. In this study, we reported similar results, with no significant difference between local inflammatory reactions in MgCA implants and titanium implants.

Owing to its molecular similarity to hydroxyapatite (HA), MgCA has been reported to have an osteoconductive ability that promotes bone healing. MgCA and HA are both calcium phosphates with comparable chemical and structural structures.(13) HA is the main mineral component of natural bone, and is responsible for its mechanical properties. MgCA has a distinct crystal structure that enables it to disintegrate and regenerate bone tissue.(14) Unlike other biomaterials, MgCA implant does not need to be coated to induce bone development.(15) In this study, we observed osteoblastic and osteoclastic activities both in titanium implant and MgCA implant.(16) Despite no significant difference between the implants, we observed higher osteoblastic activity with moderate to very severe infiltration of osteoblasts in the peri-implant area. However, despite the high activity of osteoblasts and osteoclasts surrounding the implant, the clinical significance of MgCA implants remains to be determined.

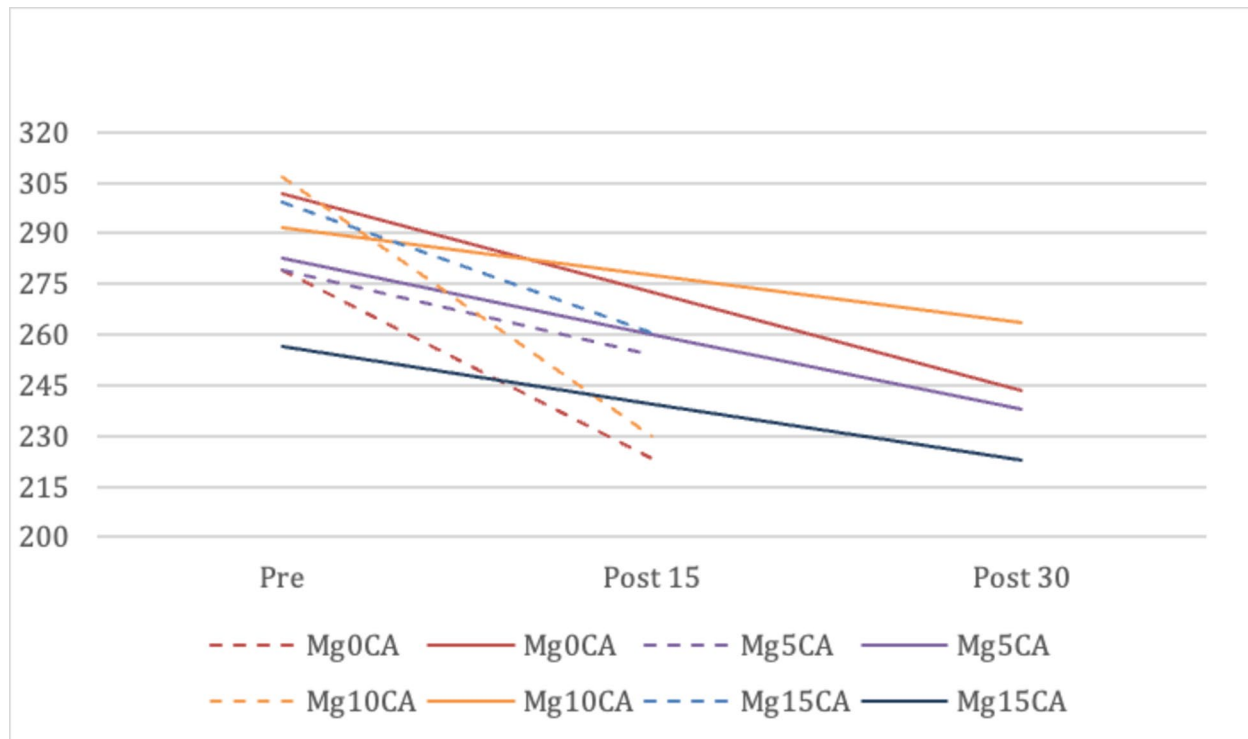


Fig. 1. Implant weight comparison.

Group	Titanium	Mg0CA	Mg5CA	Mg10CA	Mg15CA
Titanium	-	0.000	0.000	0.000	0.003
Mg0CA	0.000	-	1.000	1.000	0.116
Mg5CA	0.000	1.000	-	1.000	0.056
Mg10CA	0.000	1.000	1.000	-	1.000
Mg15CA	0.003	0.116	0.056	1.000	-

Table 5. Post-hoc analysis of the weight difference of implants in the Mg0CA, Mg5CA, Mg10CA, Mg15CA, and titanium groups post-operation.

Group	Day 1		Day 15		Day 30	
	Gas volume (mm ³)	P value	Gas volume (mm ³)	P value	Gas volume (mm ³)	P value
Titanium	0		0,000		0,000	
Mg0CA	0 (0–20,98)		12,9 (0-240,8)		0 (0-80,2)	
Mg5CA	2,2 (0-14,7)	0,090	1084,1(20,2-5350,8)	0,002	1241,2 (862,6-1393,9)	0,054
Mg10CA	26,7 (0-219,6)		53,3 (0-372,9)		0 (0-708,2)	
Mg15CA	2,6 (0-16,0)		40,7 (21,1-1256,5)		485,6 (56,01-535,6)	

Table 6. Implant gas volume. Median (min – max).

Another aspect of biocompatibility of MgCA implant is the systemic effect of the implant to other related organs.(17) In this study, we observed no significant difference in systemic organ complications between MgCA implants with various concentrations of titanium implants. Severe systemic side effects of MgCA has not been reported in prior studies other than hypersensitivity reaction to the implant.(18) In this study, histopathological examination of the kidney revealed mild non-suppurative interstitial nephritis. Kidney injury associated with the use of MgCA implants has not been described in previous studies. The presence of hyperphosphatemia has been related to the development of kidney stones that could lead to nephritis.(19) However, we did not find any significant difference in non-suppurative interstitial nephritis between titanium and MgCA; thus, the reaction could be caused by other factors.

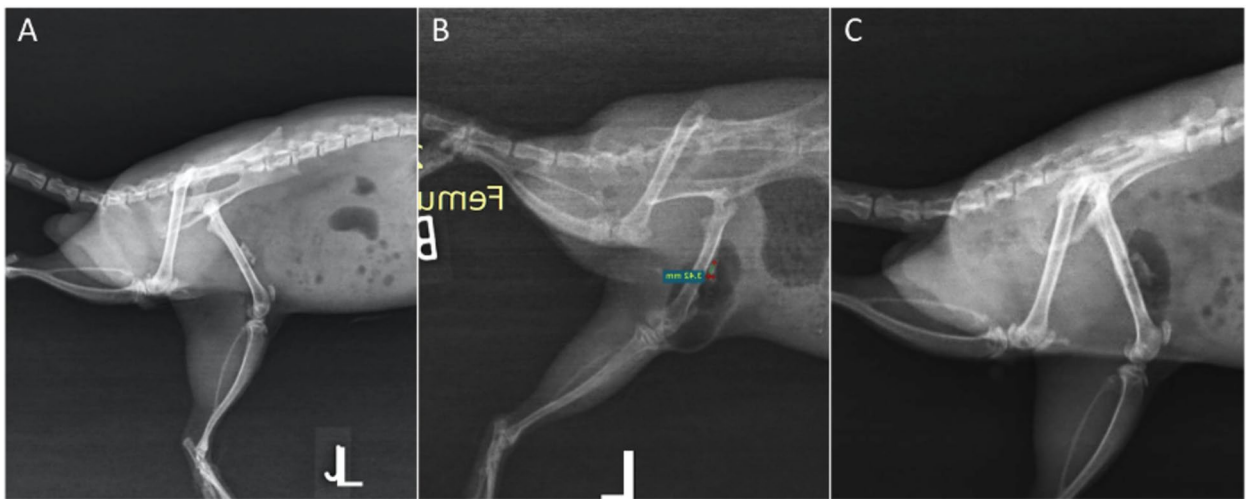


Fig. 2. Xray examination (A) immediately postoperative xray; (B) 15 days follow up Xray; (C) 30 days follow up Xray.

One of the distinct properties of MgCA implants is their ability to gradually degrade over time without the need for implant removal. While degraded inside the body, the implant reacted to the surrounding tissue, releasing magnesium and carbonate ion into the circulation while releasing hydrogen (H_2) gas into the surrounding tissue.(5) In this study, we observed degradation of the MgCA implant with the production of hydrogen gas and decreased implant weight after several weeks of observation compared to titanium implants with no hydrogen gas production. A previous study has reported that the rate of degradation and gas production of magnesium alloy is affected by the composition, microstructure, surface coating, and environmental conditions.(15) Extrusion process in the making of the implant could also affect the density of the alloy, thus affecting the rate of degradation of the implant.(9) From the results of this study, degradation of the MgCA, even though not significant, was fastest in Mg5CA Alloy. This finding is similar to in vitro finding that the addition of CA increases degradation, but higher CA (10% and 15%) content decreases degradation. (16) A similar phenomenon was found with MgHA (magnesium-hydroxyapatite) alloy, which has a similar composition to MgCA, and found that degradation decreased with the addition of HA up to MgHA 10% and then increased at 15%. (20)

In this study, we conducted the first preclinical in vivo study of MgCA alloys fabricated by extrusion as orthopedic implants to test their biocompatibility and biodegradability. We concluded that the MgCA implant fabricated by extrusion is biodegradable with low toxic properties either locally or systemically. This study is a continuation of a study of a preclinical in vitro study of MgCA by Rahyussalim et al.(21) However, we improved the processing method of the alloy mixture using the extrusion method, which allows for increased alloy density, thus overcoming the rapid degradation that occurred in a previous study. The goal of a biodegradable implant is to maintain the balance between implant degradation and implant strength to ensure fixation stability.

The shortcoming and limitation of this study is the lack of parameters to measure the biomechanical properties of the implants. We also did not analyze the surface characteristics of the implant and *scanning electron microscope* imaging of the implant after removal. Further studies should be conducted to quantify the biomechanical properties and feasibility of biodegradable implants for the treatment of fractures.

Methods

Animals

We conducted an animal study with an in vivo experimental post-test only using a control group. This study is reported in accordance with ARRIVE guidelines. Using the Federer formula, we included 30 pure breeds of male SD rats that were raised and certified by the Animal Hospital, Bogor University, Indonesia. The inclusion criteria were as follows: 12–16 weeks of age, weight 250–350 g, male sex, no abnormalities in the lower extremities, and no congenital abnormalities. The exclusion criteria were as follows: subject's death and surgical wound infection. The rats were divided into five groups, with six rats randomly allocated to each group and treated with different types of implants, including titanium implants (placebo), pure magnesium implants, 5% carbonate apatite magnesium alloy (Mg5CA), 10% carbonate apatite magnesium alloy (Mg10CA), and 15% carbonate apatite magnesium alloy (Mg15CA). The rats and implants were given random numbers, and the rats were given the corresponding implant. The caregivers, radiologists, and pathologists were blinded to the knowledge of the intervention received from each rat during the experiment, and only the lead researcher was aware of the allocation of the groups. The animals were housed randomly during the experiment. The animals were acclimatized for seven days in the animal laboratory. The animals were raised and maintained in 23 C conditions with 12 h light and dark cycles, and provided with food and water as needed (ad libitum).

After the acclimatization period, the alloy implants were surgically implanted into the rats' left femur under ketamine-HCl (80 mg/kg) and xylazine (10 mg/kg) anesthesia. The lateral approach was performed by making

a longitudinal skin incision along the anterolateral side of the femur. The incision was deepened until the lateral retinaculum was visible. The vastus lateralis and biceps femoris muscles were separated along the direction of their fibers to expose the femoral diaphysis. In each rat, a mini-plate was inserted into the left femoral diaphysis region and fixed using a multifilament vycril suture. Postoperatively, the rats were administered the oral analgesic paracetamol at a dose of 100 mg/kg BW and ampicillin antibiotic at a dose of 100 mg/kg BW for 7 days post-surgery.

The rats were observed daily for four weeks to monitor the condition of the wounds and signs of inflammation or infection. Anteroposterior (AP) and lateral radiographs were obtained from all the rats immediately after surgery to confirm the implant position. The animals were sacrificed during the fourth week by an intravenous injection of phenobarbital (10 mg/kg). This study was conducted between July 2021 and December 2021 and was approved by the Ethics Committee of the Faculty of Medicine, University of Indonesia, and Bogor Agricultural University based on the ethical approval letter number: Ethical Approval/IPB/195–2021. All procedures were performed in accordance with the relevant guidelines and regulations, as stipulated by the approved institution.

Implant preparation

MgCA implants were produced by combining commercial magnesium powder and carbonate apatite powder (varied 5, 10, and 15% wt CA) using a planetary ball mill for 5 h at 200 revolutions per minute. The mixed powder was then compacted using a die with a diameter of 1 cm by a hydraulic press with a load of 350 MPa at 350 °C in a muffle furnace. (22) After forming a cylindrical block, the sample is cut using a diamond cutter to create a mini-plate measuring 6 mm × 3 mm × 1 mm with two screw holes. The implant was prepared by the Faculty of Engineering, University of Indonesia.

Implant degradation rate

The weight of the implant was measured before implantation and after the implant was obtained from sacrificed rats. The MgCA alloy was measured in grams and compared before and after implantation to quantify the implant degeneration. The rate of degradation was also measured between the groups.

Radiographic examination

X-ray examination of the left femur was conducted 2 times for each rat, once immediately after surgery to ascertain the positioning of the implant. Additional X-rays were obtained after surgery (on days 15 and 30) to observe the degradation process and detect gas formation in the cavities.

Hematologic examination

Blood samples were collected and analyzed before and after the operation to determine the concentration of serum magnesium and calcium ions and to observe any systemic inflammatory reactions.

Histopathological examination

Histological analysis of the bone samples from each rat was conducted at the Animal Hospital Laboratory, Bogor Agricultural University, Indonesia. The bone sample was decalcified using nitric acid (HNO₃ 10%), cut into transverse sections with a thickness of 4–5 µm, and stained with Hematoxylin and Eosin (HE). Visceral organ tissue was also stained with HE. The bone samples were examined using light microscopy. A semiqualitative scoring for local reaction was created based on the level of neovascularization, level of fibrosis/fibroblast infiltration, and number of osteoblasts and osteoclasts. The scoring criteria were +0 (none/minimal), +1 (mild), +2 (moderate), +3 (severe), and +4 (very severe). (Fig. 3) The scoring was validated and performed by two pathologists in a blinded manner. Validation of the scoring system for each parameter was performed by measuring interobserver agreement using the κ value, calculated as the score agreement between observers (observer agreement) divided by 100. (23) The resulting scoring had κ values ranging from 0.84 to 0.93. Histopathological analysis of the liver, intestines, kidneys, and spleen was also performed to monitor systemic toxicity at various time points after implantation.

Statistical analysis

Statistical analysis was conducted using SPSS version 20 for Windows. The normality of the data was measured using the Shapiro-Wilk test. Repeated or one-way ANOVA will be conducted according to the normally distributed data, followed by Bonferroni or Tukey post hoc analysis. Nonparametric test will be conducted using Friedman or Kruskall Wallis analysis followed by Mann Whitney or Wilcoxon test as a post hoc analysis.

	Infiltration of Inflammatory Cells and Connective Tissue	Neovascularization	Osteoclast	Osteoblast
+ 1	"Mild fibrous tissue (>5 - 25%) in granulation tissue (magnification 40x)	Various sizes of blood vessels are found in granulation tissue with a proportion reaching >5 - 20% (magnification 40x)	The number of osteoclasts is 1-5 in the area in contact with the implant (magnification 40x)	A single layer of cuboidal-shaped osteoblast cells is found in the contact area. (magnification 40x)
+ 2	Moderate fibrous tissue (>25 - 50%) in granulation tissue. (magnification 40x)	New blood vessels of various sizes (neovascularization) are found reaching >20 - 50% (magnification 40x)	The number of osteoclasts in the contact area reaches >5 - 10 (magnification 40x)	There are two layers of cuboidal-shaped osteoblast cells at the interface area (magnification 40x)
+ 3	Thick/severe fibrous tissue (>50 - 75%), in granulation tissue (magnification 40x)	Neovascularization reaches >50 - 75% in granulation tissue (magnification 40x)	The number of osteoclasts in the contact area reaches >10 - 15	The accumulation of cuboidal-shaped osteoblast cells at the interface area reaches three layers (magnification 40x)
+ 4	Fibrous tissue reaches >75% of granulation tissue (magnification 40x).	Neovascularization reaches >75% of granulation tissue (magnification 40x)	The number of osteoclasts at the interface area reaches >15 (magnification 40x).	"The cuboidal-shaped osteoblast cells at the interface area reach more than (>3) layers of cells (magnification 40x).

Fig. 3. Local Histopathological Examination

Data availability

All data generated or analysed during this study are included in this published article [and its supplementary information files] titled ORTHOREVFFINAL.sav and Data compile biodegradable.xlsx.

Received: 3 May 2024; Accepted: 3 February 2025

Published online: 22 March 2025

References

1. Maradze, D. *et al.* High Magnesium corrosion rate has an effect on osteoclast and mesenchymal stem cell role during bone remodelling. *Sci. Rep.* **8**,10003; 10.1038/s41598-018-28476-w (2018)
2. Staiger, M.P., Pietak, A.M., Huadmai, J. & Dias, G. Magnesium and its alloys as orthopedic biomaterials: a review. *Biomaterials*. **27**, 1728–34; 10.1016/j.biomaterials.2005.10.003 (2006).
3. Doi, Y. Sintered carbonate apatites as bone substitutes. *Cells. Mater.* **7**,111–22 (1997).
4. Lou, G. *et al.* Effects of extrusion on mechanical and corrosion resistance properties of biomedical Mg-Zn-Nd-xCa alloys. *Materials (Basel)*. **12**,1049; 10.3390/ma12071049 (2019).

5. Rahyussalim, A.J. *et al.* Synthesis, structural characterization, degradation rate, and biocompatibility of magnesium-carbonate apatite (Mg-Co3Ap) composite and its potential as biodegradable orthopaedic implant base material. *J. Nanomater.* **2021**, 1–10; 10.1155/2021/6615614 (2021).
6. Milenin, A. *et al.* Microstructure and in vitro evaluation of extruded and hot drawn alloy mgca0.7 for biodegradable surgical wires. *Materials (Basel)*, **14**, 6673; 10.3390/ma14216673 (2021).
7. Antoniac, I. *et al.* Comparative assessment of in vitro and in vivo biodegradation of mg-1ca magnesium alloys for orthopedic applications. *Materials*, **14**, 84; 10.3390/ma14010084 (2021).
8. Rahman, M., Dutta, N.K. & Roy Choudhury, N. Magnesium alloys with tunable interfaces as bone implant materials. *Front. Bioeng. Biotechnol.* **8**, 564; 10.3389/fbioe.2020.00564 (2020).
9. Zeng, Z., Stanford, N., Davies, C.H.J., Nie, J.F. & Birbilis, N. Magnesium extrusion alloys: a review of developments and prospects. *Int. Mater. Rev.* **64**, 27–62; 10.1080/09506608.2017.1421439 (2019).
10. Gopi, K.R., Nayaka, H.S. & Sahu, S. Corrosion behavior of ecap-processed am90 magnesium alloy. *Arab J. Sci. Eng.* **43**, 4871–8; 10.1007/s13369-018-3203-5 (2018).
11. Rahyussalim, A.J., Supriadi, S., Kamal, A.F., Marsetio, A.F. & Pribadi, P.M. Magnesium-carbonate apatite metal composite: Potential biodegradable material for orthopaedic implant. *AIP Conf. Proceedings*. **2092**, 020021; 10.1063/1.5096689 (2019).
12. Buechel, F.F. & Pappas, M.J. Properties of materials used in orthopaedic implant systems In *Principles of Human Joint Replacement* (eds. Buechel, F.F. & Pappas, M. J.). 1–35 (Springer Berlin Heidelberg, 2011).
13. Sader, M.S., Lewis, K., Soares, G.A. & LeGeros, R.Z. Simultaneous incorporation of magnesium and carbonate in apatite: effect on physico-chemical properties. *Mater. Res.* **16**:779–84; 10.1590/S1516-14392013005000046 (2013).
14. Annur, D., Suhardi, A., Amal, M.I., Anwar, M.S. & Kartika, I. Powder metallurgy preparation of Mg-Ca alloy for biodegradable implant application Related content Powder metallurgy preparation of Mg-Ca alloy for biodegradable implant application. *J. Phys: Conf. Ser.* **817**, 012062; 10.1088/1742-6596/817/1/012062 (2017).
15. Jham, S.K., Goyal, A., Pandey, A., Marwaha, J. & Matai, J. Degradation behaviour of magnesium alloy and its composite used as a biomaterial. *E3S Web Conf.* **309**, 01085; 10.1051/e3sconf/202130901085 (2021).
16. Setyadi, I. *et al.* Fabrication of Magnesium-Carbonate Apatite by Conventional Sintering and Spark Plasma Sintering for Orthopedic Implant Applications. *Sains Malaysiana*, **51**, 883–94; 10.17576/jsm-2022-5103-22 (2022).
17. Elshahawy, W. Biocompatibility In *Advances in Ceramics - Electric and Magnetic Ceramics, Bioceramics, Ceramics and Environment* (eds. Sikalidis, C.). 359 – 78 (InTech, 2011).
18. Foussereau, J., Laugier, P. Allergic eczemas from metallic foreign bodies. *Trans. St. Johns. Hosp. Dermatol. Soc.* **52**, 220–225 (1966).
19. Prié, D., Beck, L., Silve, C., Friedlander, G. Hypophosphatemia and calcium nephrolithiasis. *Nephron. Exp. Nephrol.* **98**, e50–4; 10.1159/000080256 (2004).
20. Xiong, G., *et al.* Characterization of biomedical hydroxyapatite/magnesium composites prepared by powder metallurgy assisted with microwave sintering. *Curr. Appl. Phys.* **16**, 830–6; 10.1016/j.cap.2016.05.004 (2016).
21. Rahyussalim, A.J., Marsetio, A.F., Saleh, I., Kurniawati, T. & Whulanza, Y. The needs of current implant technology in orthopaedic prosthesis biomaterials application to reduce prosthesis failure rate. *J. Nanomater.* **2016**, 1–9; 10.1155/2016/5386924 (2016).
22. Setyadi, I., *et al.* Composite of Magnesium and Carbonate Apatite for Biodegradable Bone Implants: A Comparative Study on Sintering and Extrusion Techniques. *Int. J. Adv. Sci. Eng. Inf. Technol.* **14**, 73–80; 10.18517/ijaseit.14.1.19211 (2024).
23. Gibson-Corley, K. N., Olivier, A. K., & Meyerholz, D. K. Principles for valid histopathologic scoring in research. *Vet pathol.* **50**, 1007–1015; 10.1177/0300985813485099 (2013).

Acknowledgements

We would like to express our gratitude to all the individuals and organizations that have contributed to the publication of this research paper. We would like to thank our attending veterinarian, Arni Diana Fitri, VMD and her team for invaluable support throughout the research process and keeping the subject healthy. We are also grateful to Prima Rizky Oktari, MD, Ilham Suryo, MD and Randhi Maulana, MD for the help through the data collecting process and their valuable insights.

Author contributions

A.K., E.D., and A.R. conceived the concept and visualization, and also reviewed the manuscript. A.K., E.D., S.S., and A.R. conceived the methodology and E.D., S.S., I.S., and V.J. catered project administration and organized the resources and A.K., E.D., S.S., I.S., V.J., A.R. conducted the experiment(s), analyzed the results and conceived draft preparation and A.K. and A.R. undertook supervision.

Declarations

Competing interests

The authors declare no competing interests.

Additional information

Correspondence and requests for materials should be addressed to E.D.

Reprints and permissions information is available at www.nature.com/reprints.

Publisher's note Springer Nature remains neutral with regard to jurisdictional claims in published maps and institutional affiliations.

Open Access This article is licensed under a Creative Commons Attribution-NonCommercial-NoDerivatives 4.0 International License, which permits any non-commercial use, sharing, distribution and reproduction in any medium or format, as long as you give appropriate credit to the original author(s) and the source, provide a link to the Creative Commons licence, and indicate if you modified the licensed material. You do not have permission under this licence to share adapted material derived from this article or parts of it. The images or other third party material in this article are included in the article's Creative Commons licence, unless indicated otherwise in a credit line to the material. If material is not included in the article's Creative Commons licence and your intended use is not permitted by statutory regulation or exceeds the permitted use, you will need to obtain permission directly from the copyright holder. To view a copy of this licence, visit <http://creativecommons.org/licenses/by-nc-nd/4.0/>.

© The Author(s) 2025